Müller Cells Express the Cannabinoid CB2 Receptor in the Vervet Monkey Retina

Joseph Bouskila,[1,2] Pasha Javadi,[1] Christian Casanova,[1] Maurice Ptito,[1,3] and Jean-François Bouchard[1]*

[1]School of Optometry, University of Montreal, Montreal, Quebec, Canada H3T 1P1
[2]Biomedical Sciences, Faculty of Medicine, University of Montreal, Montreal, Quebec, Canada H3T 1P1
[3]BRAINlab, Department of Neuroscience and Pharmacology, University of Copenhagen, Copenhagen, DK-1165 Denmark

ABSTRACT

The presence of the cannabinoid receptor type 1 (CB1R) has been largely documented in the rodent and primate retinae in recent years. There is, however, some controversy concerning the presence of the CB2 receptor (CB2R) within the central nervous system. Only recently, CB2R has been found in the rodent retina, but its presence in the primate retina has not yet been demonstrated. The aim of this study was twofold: 1) to characterize the distribution patterns of CB2R in the monkey retina and compare this distribution with that previously reported for CB1R and 2) to resolve the controversy on the presence of CB2R in the neural component of the retina. We therefore thoroughly examined the cellular localization of CB2R in the vervet monkey (*Chlorocebus sabeus*) retina, using confocal microscopy. Our results demonstrate that CB2R, like CB1R, is present throughout the retinal layers, but with striking dissimilarities. Double labeling of CB2R and glutamine synthetase shows that CB2R is restricted to Müller cell processes, extending from the internal limiting membrane, with very low staining, to the external limiting membrane, with heavy labeling. We conclude that CB2R is indeed present in the retina but exclusively in the retinal glia, whereas CB1R is expressed only in the neuroretina. These results extend our knowledge on the expression and distribution of cannabinoid receptors in the monkey retina, although further experiments are still needed to clarify their role in retinal functions. J. Comp. Neurol. 521:2399–2415, 2013.

INDEXING TERMS: endocannabinoids; CB1R; CB2R; retinal glia; immunofluorescence; confocal microscopy

Anandamide (AEA) and 2-arachidonoylglycerol (2-AG) are endocannabinoids (eCBs) that bind to cannabinoid receptors (CB1R and CB2R) to exert their physiological effects (Devane et al., 1992; Mechoulam et al., 1995; Sugiura et al., 1995; Piomelli, 2003). The eCBs are endogenous lipid messengers that are involved in the regulation of many physiological processes in mammals (Di Marzo et al., 2007). They are synthesized on demand and rapidly degraded by enzymes, particularly fatty acid amide hydrolase (FAAH), monoglycerol lipase (MGL), and cyclooxygenase-2 (COX-2; Cravatt et al., 1996; Kozak et al., 2000; Dinh et al., 2002). The activation of cannabinoid receptors by eCBs leads to cannabis-like effects, and CB1R is considered to be the main element responsible for those properties. The eCB system present in the retina likely plays a role in the visual effects of cannabis (for review see Yazulla, 2008). The distribution of CB1R has been well characterized in the retina of rodents and primates (Yazulla et al., 1999; Straiker et al., 1999; Bouskila et al., 2012). It is present in cone pedicles and rod spherules, bipolar cells, amacrine cells, horizontal cells, and ganglion cells. This pattern is also observed in the central and peripheral parts of the monkey retina (Bouskila et al., 2012).

With regard to CB2R, its mRNA was first detected by reverse transcription polymerase chain reaction (RT-PCR) in the adult mouse retina and by in situ hybridization in the adult rat retina (Lu et al., 2000) but not in rat embryos (Buckley et al., 1998). Interestingly, with different transcripts, CB2 mRNA was not detected in

Grant sponsor: Natural Science and Engineering Research Council of Canada; Grant number: 311892-2010 (to J.-F.B.); Grant number: 6362-2012 (to M.P.); Grant number: 194670-2009 (to C.C.); Grant sponsor: Canadian Institutes of Health Research; Grant number: MOP-86495 (to J.-F.B.).

*Correspondence to: Jean-François Bouchard, BPharm, PhD, School of Optometry, Room 260-7, 3744 Jean-Brillant, University of Montreal, Montreal, Quebec, Canada H3T 1P1. E-mail: jean-francois.bouchard@umontreal.ca

Received November 1, 2012; Revised March 8, 2013;
Accepted for publication March 13, 2013.
DOI 10.1002/cne.23333
Published online April 29, 2013 in Wiley Online Library (wileyonlinelibrary.com)

rat and human retinae (Porcella et al., 1998, 2000). In agreement with the work of Lu et al. (2000), using immunohistochemistry, CB2R protein was localized in rat retinal pigment epithelium, inner photoreceptor segments, horizontal and amacrine cells, cells localized in the ganglion cell layer, and fibers of the inner plexiform layer (López et al., 2011). However, this study did not proceed by double labeling with specific retinal cell markers. Instead, cell types were identified based on the position in the retinal layer and on the morphology of the cells. CB2R expression was found in the trabecular meshwork of the porcine eye, in which an injection of a CB2R agonist increased aqueous humor outflow (Zhong et al., 2005). The presence of both CB1R and CB2R has been reported in human retinal pigment epithelial cells in primary cultures and ARPE-19 cells (Wei et al., 2009). Recently, CB2R expression was found at mRNA levels by RT-PCR and protein by Western blot analysis in in vitro retinal explants and primary cultures of human Müller glia (Krishnan and Chatterjee, 2012).

The human CB2R was cloned first (Munro et al., 1993). Subsequent studies on CB2R expression patterns focused on the presence of CB2R in peripheral tissues of the immune system (Galiègue et al., 1995). Later, CB2R was cloned in the mouse (Shire et al., 1996) and rat (Griffin et al., 2000). Unlike CB1R, which is highly conserved across mammalian species, sequences of the murine and human CB2R are divergent, raising the possibility of species-specific amino acid sequences. Indeed, CB2R has evolved far more rapidly (McPartland et al., 2007), such that there is only an 81% sequence homology at the amino acid level between the rat and human CB2R, increasing to 87% identity in the critical transmembrane regions (Griffin et al., 2000). As a result, rodent models may not reliably predict the performance of a CB2R agonist for human CB2 receptors (Mackie, 2008). Consequently, accurate comparisons between human and rodent receptors are crucial, given that cannabinoids vary in their affinity for CB2R, depending on the species (Mukherjee et al., 2004). Our study fills an important gap in knowledge of the expression patterns of CB2R in the retina.

The presence of CB2R in neurons has raised an important debate in the scientific community (Atwood and Mackie, 2010). Some are convinced that CB2R is not present in neurons, or at least at very low levels (Atwood and Mackie, 2010); others suggest otherwise (Onaivi et al., 2012). Nevertheless, all agree that CB2R is present in the CNS and could be expressed in its glial elements. Despite extensive knowledge of the distribution of CB2R in the rodent brain, there are no published reports regarding its expression and localization in the human and monkey retinae. Given that endocannabinoids are present in human ocular tissues, especially the retina (Chen et al., 2005), it is reasonable to assume the presence of cannabinoid receptors therein. Therefore, the main objective of this study is to characterize the expression and localization patterns of CB2R throughout the in vivo monkey retina.

MATERIALS AND METHODS

Choice of species

Monkey tissue, the experimental model for the current study, was chosen for several reasons. Monkey tissue allows us to generalize more easily to humans. The anatomical similarity between the monkey and human retina is remarkable. Primates are mammals that have a macular/foveal region and multiple cone types, which offers them high visual acuity and color vision. Finally, the high cross-reactivity between human and monkey antigens increases chances of success for targeting CB2R in monkeys using an anti-human CB2R antibody.

Animal preparation

Three adult vervet monkeys (*Chlorocebus sabeus*) were used for this study. Monkey tissues were kindly provided by Prof. Roberta Palmour from McGill University. The monkeys were part of Dr. Palmour's and Dr. Ptito's research project that was approved by the McGill University Animal Care and Use Committee. The animals were born and raised in enriched environments in the laboratories of the Behavioural Sciences Foundation (St.-Kitts, West Indies) that is recognized by the Canadian Council on Animal Care (CCAC). The animals were fed with primate chow (Harlan Teklad High Protein Monkey Diet; Harlan Teklad, Madison, WI) and fresh local fruits, with water available ad libitum. The experimental protocol was reviewed and approved by the local Animal Care and Use Committee and the Institutional Review Board of the Behavioural Science Foundation. Each animal was sedated with ketamine (10 mg/kg, i.m.), deeply anesthetized with sodium pentobarbital (25 mg/kg, i.v.), and perfused transcardially with phosphate-buffered saline (PBS 0.1M; pH 7.4), followed by 4% paraformaldehyde.

Antibody characterization

All the primary antibodies used in this work, their sources, and their working dilutions, are summarized in Table 1. These antibodies were successfully used in previous studies and are well characterized with regard to the specific primate retinal cell type immunostaining, as described below for each antibody.

Glutamine synthetase

The mouse monoclonal (IgG2a) to glutamine synthetase (GS) was obtained from Chemicon (Temecula, CA) and

TABLE 1.
Primary Antibodies Used in This Study

Antibody*	Immunogen	Source†	Working dilution
GS	Full protein purified from sheep brain	Chemicon, Temecula, CA; MAB302, mouse monoclonal, clone GS-6	H: 1:500
CB	Purified bovine kidney calbindin-D28K	Sigma, St. Louis, MO; C9848, mouse monoclonal, clone CB-955	H: 1:250
PKCα	Peptide mapping the aa 296–317 of human PKCα	Santa Cruz Biotechnology, Santa Cruz, CA; sc-8393, mouse monoclonal, clone H-7	H: 1:500
PV	Full protein purified from frog muscle	Sigma, St. Louis, MO; P3088, mouse monoclonal, clone PARV-19	H: 1:250
Syntaxin	Synaptosomal plasma fraction of rat hippocampus (Barnstable et al., 1985)	Sigma, St. Louis, MO; S0664, mouse monoclonal, clone HPC-1	H: 1:500
Brn3a	Fusion protein containing aa 186–224 of Brn3a protein	Chemicon, Temecula, CA; MAB1585, mouse monoclonal, clone 5A3.2	H: 1:100
CB1R	Fusion protein containing aa 1–77 of rat CB1R	Sigma, St. Louis, MO; C1233, rabbit polyclonal	H: 1:150
CB2R	Synthetic peptide corresponding to aa 20–33 of human CB2R	Cayman Chemical, Ann Arbor, MI; 101550, rabbit polyclonal	H: 1:150 W: 1:500
Kir4.1	Synthetic peptide corresponding to aa 352–368 of human Kir4.1	Osenses, Keswick, South Australia; OSP00134W, goat polyclonal	H: 1:500
GAPDH	Full-length rabbit muscle GAPDH protein	Sigma, St. Louis, MO; G8795, mouse monoclonal, clone GAPDH-71.1	W: 1:20,000

*GS, glutamine synthetase; CB, calbindin; PKCα, protein kinase C (α isoform); PV, parvalbumin; CB1R, cannabinoid receptor type 1; CB2R, cannabinoid receptor type 2; GAPDH, glyceraldehyde-3-phosphate dehydrogenase; aa, amino acids; H, immunohistochemistry; W, Western blot.
†The source column indicates the commercial company, catalog reference and origin. The clone designation is given for monoclonal antibodies.

directed against GS purified from sheep brain. This antibody generates a single 45-kDa band in immunoblots of adult mammalian brain tissue (manufacturer's data sheet). This antibody labels Müller cells in rat (Riepe and Norenburg, 1977) and monkey retinae (Nishikawa and Tamai, 2001; Bouskila et al., 2012).

Calbindin

The mouse monoclonal (IgG1) to calbindin (CB) was obtained from Sigma (St. Louis, MO) and directed against purified bovine kidney calbindin-D-28K. This antibody recognizes a 28-kDa band on Western blots (manufacturer's data sheet). The CB antibody labels cones outside the foveal region, cone bipolar cells, and a subset of horizontal cells in human and monkey retinae (Fischer et al., 2001; Chiquet et al., 2002; Kolb et al., 2002; Martínez-Navarrete et al., 2007, 2008; Bouskila et al., 2012).

Protein kinase C

The mouse monoclonal (IgG2a) to protein kinase C (PKC) was developed by Santa Cruz Biotechnology (Santa Cruz, CA) by using as immunogen purified bovine PKC, and its epitope is mapped to its hinge region (amino acids 296–317). It detects the PKCα isoform, a well-known specific marker for rod bipolar cells (Mills and Massey, 1999). As stated by the manufacturer, this antibody gives a single band of 80-kDa on Western blots of human cell lines and has been previously used for immunohistochemistry on rodent (Zabouri et al., 2011a,b) and monkey (Cuenca et al., 2005; Martínez-Navarrete et al., 2008; Bouskila et al., 2012) retinae.

Parvalbumin

The mouse monoclonal (IgG1) to parvalbumin (PV) was obtained from Sigma (St. Louis, MO) by using as immunogen purified frog muscle PV. It recognizes a 12-kDa band from human, bovine, pig, canine, feline, rabbit, rat, and fish tissues (manufacturer's technical information). The pattern of labeling with this antibody was the same as reported previously (Kolb et al., 2002; Bordt et al., 2006). This small calcium-binding protein is expressed in the primate retina by horizontal cells (Wässle et al., 2000), and the antiserum has been used to visualize monkey thalamic nuclei (Qi et al., 2011).

Syntaxin

The mouse monoclonal (IgG1) to syntaxin (clone HPC-1) was developed by Barnstable et al. (1985) and is distributed by Sigma. This antibody recognizes syntaxin-1, a 35-kDa protein, from hippocampal, retinal, and cortical neurons (Inoue et al., 1992) and labels horizontal cells and amacrine cells in the developing and adult human retina (Nag and Wadhwa, 2001). The staining pattern obtained in the current study was similar to that found in human retina (Nag and Wadhwa, 2001). We have used this antibody to label monkey retinal amacrine and horizontal cells (Bouskila et al., 2012).

Brn3a

The mouse monoclonal (IgG1) to Brn3a was obtained from Chemicon and made against amino acids 186–224 of Brn3a fused to the T7 gene 10 protein. The Brn3a antibody shows no reactivity to Brn3b or Brn3c by Western blot and no reactivity to Brn3a knockout mice (manufacturer's technical information). Its specificity for rodent (Nadal-Nicolás et al., 2009) and monkey (Xiang et al., 1995) retinal ganglion cells has been documented. We used the POU-domain transcription factor Brn3a to label the nuclei of retinal ganglion cells (Bouskila et al., 2012).

CB1R

The rabbit anti-CB1R was obtained from Sigma. It was developed by using a highly purified fusion protein containing the first 77 amino acid residues of the rat CB1R as the immunogen. It recognizes a major band of 60-kDa and less intense bands of 23, 72, and 180-kDa (manufacturer's data sheet; C1233). This antibody targets the rat CB1R (Zabouri et al., 2011a) but specifically recognizes the CB1R (60-kDa) from many species (manufacturer's data sheet), including vervet monkey retinal tissue (Bouskila et al., 2012).

CB2R

The rabbit anti-CB2R was obtained from Cayman Chemical (Ann Arbor, MI). It was developed by using a synthetic peptide corresponding to the amino acids 20–33 (NPMKDYMILSGPQK) of the human CB2R sequence conjugated to keyhole limpet hemocyanin (KLH) as immunogen. This antibody recognizes a band at 45-kDa and a band at 39–40-kDa (manufacturer's data sheet; 101550). This antibody was used in human nervous tissues (Ellert-Miklaszewska et al., 2007; Zurolo et al., 2010). Its specificity to CB2R was recently validated in CB2R knockout mouse retinal tissue. CB2R immunohistochemistry signal present in CB2R wild-type mice was completely absent in their knockout littermates (Argaw et al., 2011).

Glyceraldehyde-3-phosphate dehydrogenase

The mouse monoclonal antibody (IgM) to glyceraldehyde-3-phosphate dehydrogenase (GAPDH; clone GAPDH-71.1) was obtained from Sigma by using as immunogen purified rabbit muscle GAPDH (whole molecule). As stated by the manufacturer, this antibody recognizes monkey GAPDH and gives a single band at about 37-kDa.

Kir4.1

The goat polyclonal anti-Kir4.1 was purchased from Osenses (Keswick, South Australia, Australia). This antibody was raised against a synthetic peptide corresponding to amino acids 352–368 (PEKLKLEESLREQAEKE) of human KCNJ10 (Kir4.1) conjugated to an immunogenic carrier protein and gives a single band at about 37-kDa in Western blot. The peptide is homologous in mouse and rat and was predicted to react in rat, mouse, and human tissues (manufacturer's technical information; OSP00134W). It has been characterized by immunoblotting and immunostaining of HEK cells transfected with Kir4.1 and used to target the Kir4.1 in mouse cortical astrocytes (Li et al., 2001).

CB2R blocking peptide

The CB2R blocking peptide containing the human CB2R amino acid sequence 20–33 (NPMKDYMILSGPQK; Cayman Chemical; 301550) was used in the present study for immunohistochemistry and Western blot analysis. The specificity of the CB2R antibody was also tested by preincubation with the corresponding blocking peptide. For preadsorption, the primary antibody was diluted in PBS and incubated with a ratio 1:1 for 2 hours at room temperature, with occasional inversion. Thereafter, the antibody-blocking peptide solution was added to the slices and subsequent immunohistochemistry followed the protocol as described further.

Tissue preparation

The eyes were extracted, and the retina was dissected free from the eyecup in a PBS bath. The retina was laid flat so that the vitreous body could be removed by blotting with filter paper and gentle brushing (Burke et al., 2009). Samples of retina (4 mm^2) were taken from the center (radius of 4 mm around the fovea), middle (radius of 10 mm around the fovea), and periphery (radius of 20 mm around the fovea), along with the fovea. Each sample was cryoprotected in 30% sucrose overnight and embedded in Shandon embedding media at −65°C. Retinal samples were sectioned in a cryostat (18 μm) and mounted onto gelatinized glass microscope slides, air dried, and stored at −20°C.

Western blotting

To test the specificity of the CB2R antisera, Western blots were performed on monkey tissue. A freshly dissected sample of retina, visual cortex, or cerebellum was homogenized by hand by using a sterile pestle in RIPA buffer (150 mM NaCl, 20 mM Tris, pH 8.0, 1%, NP-40 [USB Corp., Cleveland, OH], 0.1% SDS, 1 mM EDTA), supplemented with a protease-inhibitor mixture (aprotinin [1:1,000], leupeptin [1:1,000], pepstatin [1:1,000], and phenylmethylsulfonyl fluoride [0.2 mg/ml]; Roche Applied Science, Laval, Quebec, Canada). Samples were centrifuged at 4°C for 10 minutes, and the supernatant was extracted and stored at −20°C until further processing. Protein content was equalized by using a Thermo Scientific Pierce BCA

Protein Assay Kit (Fisher Scientific, Ottawa, Ontario, Canada). Thirty micrograms of protein/sample of the homogenate was resolved with 10% sodium dodecyl sulfate (SDS)-polyacrylamide gel electrophoresis, transferred onto a nitrocellulose membrane filter (BioTrace NT; Life Sciences, Pall, Pensacola, FL), blocked for 1 hour in 5% skim milk (Carnation, Markham, Ontario, Canada) in TBST (0.15 M NaCl, 25 mM Tris-HCl, 25 mM Tris, 0.5% Tween-20), and incubated overnight with the primary antibody, namely, rabbit anti-CB2R (1:500), in blocking solution. On the following day, the blot was exposed to a secondary antibody conjugated to horseradish peroxidase (1:5,000; Jackson Immunoresearch, West Grove, PA) in blocking solution for 2 hours. Detection was carried out by using homemade ECL Western blotting detection reagents (final concentrations 2.50 mM luminol, 0.4 mM p-coumaric acid, 0.1 M Tris-HCl, pH 8.5, 0.018% H_2O_2). The membrane was then air stripped, reblocked, and exposed to a second primary antibody, namely, mouse anti-GAPDH (1:20,000), until all proteins of interest had been tested. Densitometric analysis was performed in ImageJ software (version 1.45; http://rsb.info.nih.gov/ij/) on scanned films.

Immunohistochemistry

Single, double, and triple labeling of the retina were performed according to previously published methods (Bouskila et al., 2012). Briefly, sections were postfixed for 5 minutes in 70% ethanol; rinsed for 3 × 5 minutes in 0.1 M Tris buffer, pH 7.4, 0.03% Triton; and blocked for 90 minutes in 10% Normal Donkey Serum (NDS) in 0.1 M Tris buffer/0.5% Triton. Sections were incubated overnight at room temperature with primary antibody in blocking solution. The CB2R antibody was used conjointly with a known retinal cell type marker: calbindin, PKCα, syntaxin, Brn3a, or glutamine synthetase (Table 1). On the next day, sections were washed for 10 minutes and 2 × 5 minutes in 0.1 M Tris/0.03% Triton, blocked in 10% NDS, 0.1 M Tris/0.5% Triton for 30 minutes and incubated with secondary antibody for 1 hour: Alexa 488 donkey anti-mouse, Alexa 488 donkey anti-goat, Alexa 555 donkey anti-mouse or biotinylated donkey anti-rabbit followed by the addition of streptavidin–Alexa 647 (1:200), all in a blocking solution as described above. Sections were washed again in Tris buffer; counterstained with bisbenzimide (Hoechst 33258; Sigma; 2.5 μg/ml), a fluorescent nuclear marker; and coverslipped with Fluoromount-G Mounting Medium (Southern Biotechnology, Birmingham, AL).

Sequential labeling of CB1R and CB2R

The CB1R and CB2R antibodies that we selected came from the same host, making the use of simultaneous double-labeling protocol inadequate. To circumvent this problem, we used a sequential protocol previously described by our research group (Zabouri et al., 2011a,b; Bouskila et al., 2012). Briefly, the sections were labeled in a serial manner. The exposure to the first primary antibody was conducted as described above, followed by incubation of a goat anti-Fab fragment solution (Jackson Immunoresearch); Brandon, 1985). This allowed for the tagging of the first primary antibody as goat rather than rabbit. The sections were revealed with a secondary Alexa donkey anti-goat 488. Thereafter, they were exposed to a second primary antibody overnight and revealed on the following day with an Alexa donkey anti-rabbit 647. The validity of the sequential staining was then verified for CB1R/CB2R colabeling with the following two controls: 1) omission of the second primary antibody, resulted in a strong staining with the goat secondary 488 but no staining with rabbit secondary 647, and 2) omission of the first secondary and second primary antibodies, revealing faint signal for the goat secondary 488 and no signal for the rabbit secondary 647.

Confocal microscopy

Fluorescence was detected with a Leica TCS SP2 confocal laser scanning microscope (Leica Microsystems, Exton, PA), using a ×40 (n.a. 1.25–0.75) or a ×100 (n.a. 1.40–0.7) objective. Images were obtained sequentially from the green and far-red channels on optical slices of less than 0.9 μm thickness. Throughout the Results section, images taken from the green channel correspond to the retinal cell markers and from the far-red channel to CB2R. When coexpression of CB2R and retinal cell markers was ambiguous in some retinal layers, colabeling or its absence was demonstrated by taking z-stacks with optimized steps. This allowed for visualization of the cells in the X–Y, X–Z, and Y–Z axes, thereby confirming the presence or absence of CB2R in the cells. All photomicrographic adjustments, including size, color, brightness, and contrast, were performed in Adobe Photoshop (CS5; Adobe Systems, San Jose, CA) and then exported to Adobe InDesign (CS5; Adobe Systems), where the final figure layout was completed. The schematic panels of Figure 9 were created in Adobe Illustrator (CS5; Adobe Systems).

RESULTS

CB2R antibody specificity

Immunoblots of CB2R antisera in homogenates of fresh vervet monkey retina, visual cortex, and cerebellum (Fig. 1A) showed one intense band at 45-kDa for each homogenate. Preincubation with CB2R blocking

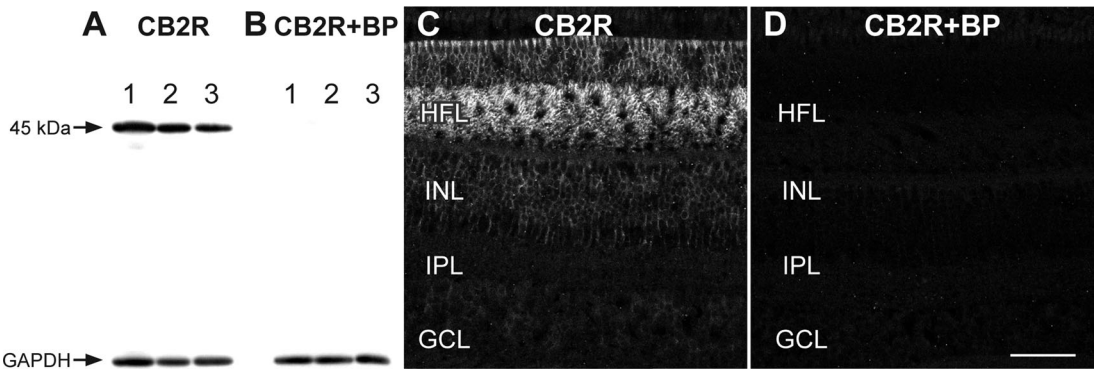

Figure 1. Characterization of CB2R antibody in the vervet monkey. Western blot analysis of total protein samples from retina (**A**, lane 1), visual cortex (A, lane 2), and cerebellum (A, lane 3) showing detection of one heavy protein band at 45 kDa. The band was not detected when the antibody was preincubated with the corresponding CB2R blocking peptide (BP; **B**, lanes 1–3). All lanes contained 10 μg of total protein. The lower blots for CB2R and CB2R-BP show the expression of the protein GAPDH and demonstrate loading in all lanes. Immunohistochemistry on vervet retinal tissue with the anti-CB2R antibody revealed a unique staining profile (**C**). When the CB2R antibody was preincubated with its BP, this revealed an absence of staining (**D**). HFL, Henle fiber layer; INL, inner nuclear layer; IPL, inner plexiform layer; GCL, ganglion cell layer. Scale bar = 75 μm.

peptide completely abolished antibody signal (Fig. 1B). The same blot was reprobed using the GAPDH antibody (37-kDa) to ensure the proper equalization and loading of all samples (Fig. 1A, B, lower panels). As an added control, the CB2R antibody was preadsorbed with its blocking peptide prior to incubation with retinal sections, resulting in an absence of staining signal in the section (Fig. 1D; see CB2R blocking peptide paragraph in Materials and Methods). Furthermore, the CB2R knockout mice validated the specificity of anti-CB2R by elimination of the immunolabeling (Argaw et al., 2011). CB2R immunoreactivity (IR) was present throughout the monkey retina, extending from the fovea centralis to the periphery and from the external limiting membrane to some cell bodies of the inner nuclear layer (Fig. 1C). CB2R was densely expressed in the Henle fiber layer (Fig. 1C), comprising the cone photoreceptor oblique axons with accompanying Müller glial cell processes and forming a pale-staining fibrous-looking area not seen in the peripheral retina (Fig. 3H).

CB2R immunoreactivity throughout the monkey retina

The expression pattern of CB2R near the fovea and in the peripheral retina seems different on visual examination, but this is misleading, because Müller cells have different morphological characteristics in the central and peripheral retina (Distler and Dreher, 1996). If one looks at the pattern of Müller cell processes, CB2R distributions are rather similar. The strongest CB2R signal is localized in the Henle fiber layer with generally weaker signals in the inner retina (Fig. 2).

Double-label immunohistochemistry

To verify the retinal cell type expression, double immunostaining was carried out for CB2R and a specific molecular marker for primate retinal cells. A consistent staining pattern across all three monkey retinae was found for each double staining. Although labeling was located in all distal layers of the retina, from the photoreceptor to the inner nuclear layers, CB2R-IR was most prominent in the Henle Fiber layer within the central retina (see Figs. 3, 5, 6, 9).

Cellular distribution of CB2R

CB2R is present in Müller cells

The extensive CB2R-immunoreactive fibers along the external limiting membrane were suggestive of Müller cells (Fig. 3A–C). This hypothesis was tested by double labeling CB2R-IR with GS-IR, which labels Müller cells in the mammalian retina, including vervet monkey retina (Riepe and Norenburg, 1977; Bouskila et al., 2012). All fibers that were GS-immunoreactive were also double labeled for CB2R-IR in the central retina (Fig. 3D–F) and in the middle retina (Fig. 3G–I). This included all the Müller cell fibers but not Müller cell bodies (Fig. 3A–C). Most prominent staining was found in the distal retina, with only faint staining in the proximal retina. On occasion, some GS-immunoreactive proximal fibers were not CB2R immunoreactive. Villous processes extending beyond the external limiting membrane (arrows) did not colocalize with CB2R-IR.

No expression of CB2R in cones

Because the Henle fiber layer comprises densely packed oblique cone photoreceptor axons with accompanying

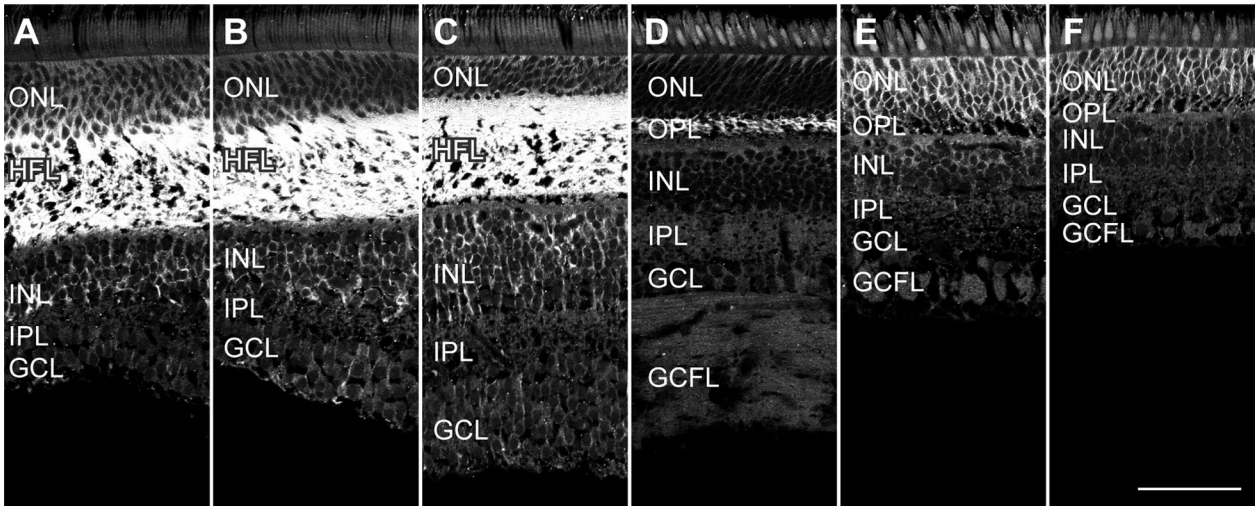

Figure 2. Labeling pattern of CB2R-IR throughout the monkey retina. Confocal micrographs taken from the fovea (**A**) and from 1 mm (**B**), 2 mm (**C**), 5 mm (**D**), 10 mm (**E**), and 20 mm (**F**) of the fovea. Note that the most prominent staining of CB2R is located in the Henle fiber layer present in samples of central retina. ONL, outer nuclear layer; HFL, Henle fiber layer; OPL, outer plexiform layer; INL, inner nuclear layer; IPL, inner plexiform layer; GCL, ganglion cell layer; GCFL, ganglion cell fiber layer. Scale bar = 75 μm.

Müller cell processes, CB2R and CB colocalization was needed to rule out the possibility that CB2R was present in cones. Given that CB labels cones outside the foveola, central (Fig. 4A–C) and middle (Fig. 4D–F) retinal samples were taken to perform colocalization with CB2R and CB. Although the patterns of CB2R-IR throughout the ONL and OPL appeared very similar to those of GS-IR, it was not clear from an overlay projection presented in Figure 4 that CB2R-IR is truly adjacent to cone axons. A flattened Z-series indicated that CB2R-IR in the ONL was due exclusively to fibers of the Müller cells and did not include cone axons (Fig. 4G). To corroborate the localization of CB2R in GS-positive fibers, but not in CB-positive axons, confocal optical sections were investigated in the X–Z and Y–Z projections. The X–Z and Y–Z images were drawn through the point of double labeling between CB-IR and CB2R-IR, and the two orthogonal views clearly show no overlap (Fig. 4H).

CB2R is not present in rod bipolar cells

Occasionally, there were CB2R-immunoreactive cell fibers in the proximal INL that looked like PKC-immunoreactive rod bipolar cell axons in the central retina (Fig. 5A–C) and peripheral retina (Fig. 5D–F). No PKC-immunoreactive rod bipolar cell, including its cell body, axon, and axon terminal, was colocalized with CB2R-IR, confirming that CB2R-IR was not present in rod bipolar cells.

Horizontal cells do not express CB2R

CB2R-IR did not colocalize with PV-IR in the central retina (Fig. 6A–C) and peripheral retina (Fig. 6D–F), indicating that horizontal cells were not CB2R immunoreactive. The PV-IR is classically associated with equal staining of two morphological types of horizontal cells in the primate retina (arrows), H1 and H2 horizontal cells (Röhrenbeck et al., 1987), and no clear colocalization was found in any horizontal cells of the vervet monkey retina (Fig. 6A–F).

CB2R is not present in amacrine cells

The monoclonal antibody HPC-1 that recognizes syntaxin in horizontal and amacrine cells was used to evaluate CB2R-IR expression in amacrine cells (Fig. 7A–C). Despite variations in intensity of immunolabeling, virtually no amacrine cells showed expression of CB2R-IR in the central retina (Fig. 7D–F) or the middle retina (Fig. 7G–I). Although there was no visible expression of CB2R in horizontal cells (arrows) and amacrine cells (arrowheads), the staining found in the layers of horizontal and amacrine cells was limited to the Müller cell processes (Fig. 7B, E).

CB2R is absent in ganglion cells

Brn3a immunoreactivity specifically labels retinal ganglion cell nuclei. CB2R-IR was not detected in ganglion cell bodies (arrowheads) either in the central (Fig. 8A–C) or in the middle (Fig. 8D–F) retina. Displaced Brn3a-positive cells located in the IPL were not CB2R immunoreactive (arrows). Double labeling with Brn3a/CB2R showed that CB2R was not expressed in ganglion cells.

Differential CB1R and CB2R labeling

Double labeling of CB1R-IR and CB2R-IR was performed in a retinal sample of 2 mm eccentricity from

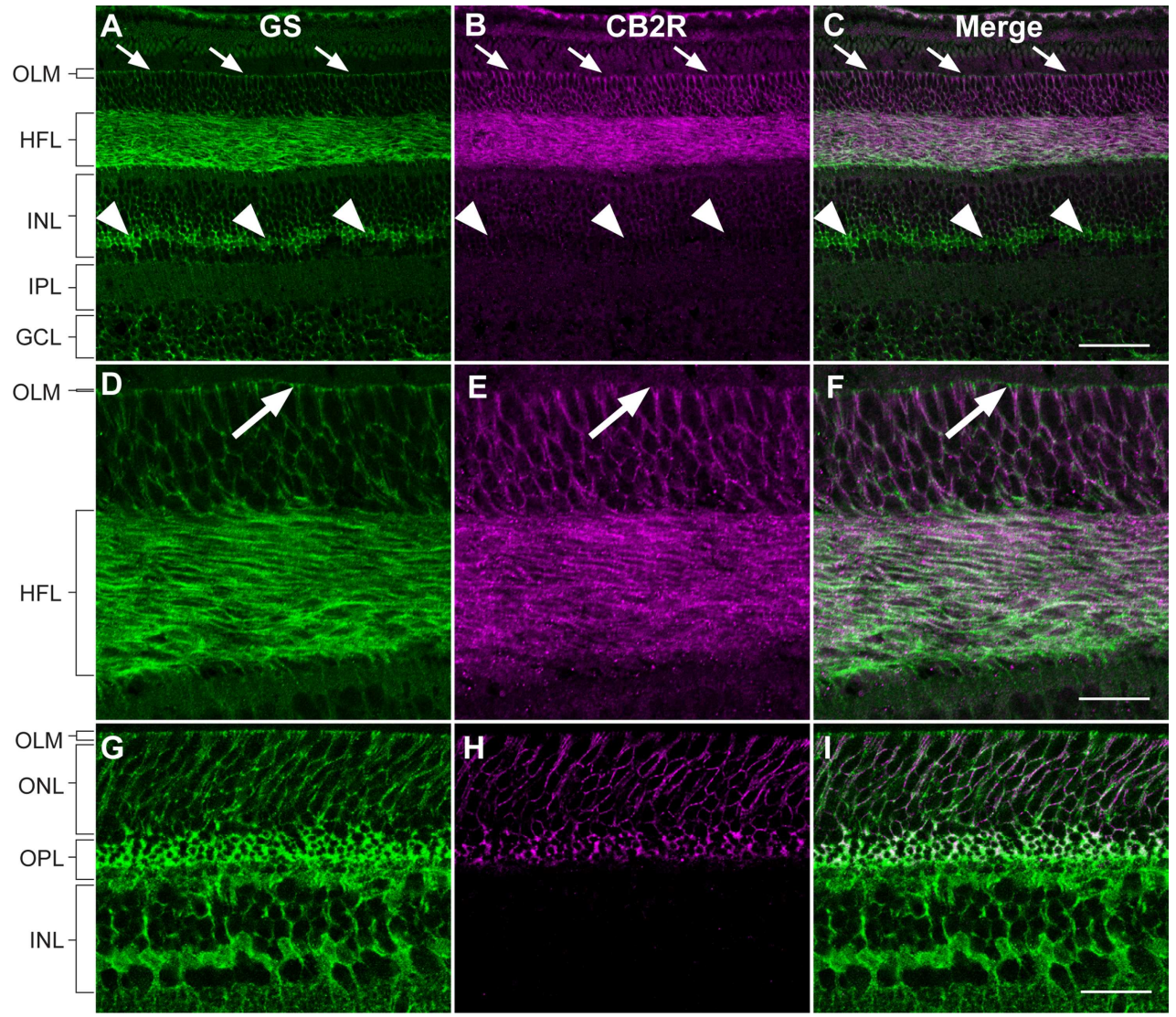

Figure 3. CB2R colocalizes extensively with glutamine synthetase-labeled Müller cells in the monkey retina. A–I: Vertical sections taken near the fovea (**A–F**) and in the middle retina (**G–I**). Confocal micrographs of retinae coimmunolabeled for CB2R and glutamine synthetase (GS), a cell-type-specific marker for Müller cells. Each protein is presented alone in the first columns. The merged image is presented in the last column (GS in green and CB2R in magenta). Arrows indicate the projections of the Müller cell membrane in the apical margin known as apical villi that lack CB2R. Arrowheads point to Müller cell bodies that do not express CB2R. D–F: Higher magnification views of the outer limiting membrane (OLM) demonstrate the absence CB2R/GS double labeling in the Müller cell villi. OLM, outer limiting membrane; HFL, Henle fiber layer; INL, inner nuclear layer; IPL, inner plexiform layer; GCL, ganglion cell layer. Scale bars = 75 μm in C (applies to A–C); 30 μm in F (applies to D–F); 30 μm in I (applies to G–I). [Color figure can be viewed in the online issue, which is available at wileyonlinelibrary.com]

the fovea (Fig. 9A–C) and 6 mm eccentricity from the fovea (Fig. 9J–L) to differentiate the localization of these cannabinoid receptors. There was no large overlap in the expression of these two receptors in the ONL, INL, IPL, and GCL but apparent overlap was seen in the HFL. Detailed expression of CB1R for each cell type has been previously characterized (Bouskila et al., 2012), and precise expression of CB2R is presented in Figures 3–8. Note that, for the most part, CB1R expression is found throughout the retinal neurons of the monkey retina and CB2R in the retinal Müller cells. To distinguish CB1R-IR from CB2R-IR in the HFL, a 6-mm eccentricity sample of the monkey retina was taken, because the HFL is present only in the central retina close to the fovea. Figure 9A–C shows immunostaining for the complete protocol, in which strong signals for both CB1R (Fig. 9A) and CB2R (Fig. 9B) can be seen. Figure 9D–F illustrates the first control in which the second primary antibody was omitted: a clear signal for CB1R (Fig. 9D), with no staining for CB2R (Fig. 9E).

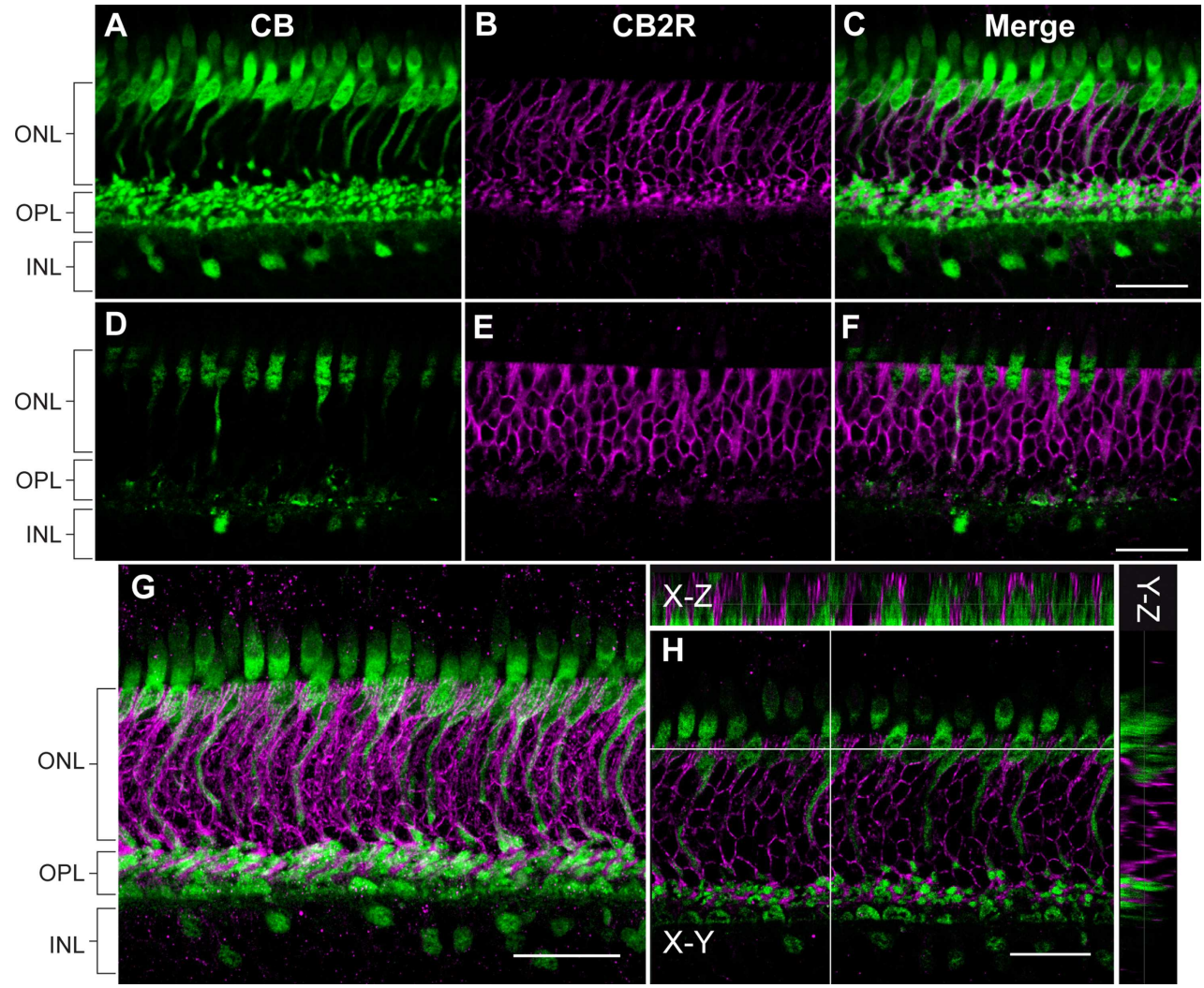

Figure 4. Double-label immunofluorescence illustrating localization of calbindin (CB) and CB2R. **A–C:** Calbindin-IR labeled cone photoreceptors in the monkey central retina, and these were not CB2R immunoreactive. Note that CB2R-IR appears colocalized in the ONL, but a flattened Z-series (**G**) and a 3D reconstruction in the X–Z and Y–Z axes showed no colocalization (**H**). CB2R-IR was not present throughout cones outside of the central region, as illustrated in the overlay of the two micrographs (**D–F**). This overlay clearly shows that the CB2R-immunoreactive outer processes were neighboring the CB-immunoreactive cone photoreceptors. ONL, outer nuclear layer; OPL, outer plexiform layer; INL, inner nuclear layer. Scale bars = 75 μm in C (applies to A–C); 75 μm in F (applies to D–F); 75 μm in G, H. [Color figure can be viewed in the online issue, which is available at wileyonlinelibrary.com]

Figure 9G–I presents the results for the second control, in which the first secondary and second primary antibodies were omitted: there was no staining for CB1R (Fig. 9G) or CB2R (Fig. 9H). Figure 9J–L clearly shows no colocalization of CB1R (Fig. 9J) and CB2R (Fig. 9K) in the outer retina. Arrowheads follow a CB1R-positive cone cell body and axon; note that CB2R-positive Müller cell processes envelop this cone. These data are summarized in Figure 10A for all retinal cell types.

Triple labeling of CB2R, GS, and Kir4.1

Triple-immunofluorescent labeling was performed to verify whether potassium channels colocalize with CB2R in Müller cells. Expression of Kir4.1 was found in CB2R-positive and GS-positive Müller cells of the central retina. Coexpression of CB2R and Kir4.1 was found in the HFL but scarcely in the proximal parts of Müller cells (Fig. 11A–D). There was a large overlap in the expression of GS and Kir4.1 in the INL, IPL, and GCL (Fig. 11E–L).

DISCUSSION

This article reports the presence of CB2R in Müller cells of the vervet monkey retina. These findings are important because, although the presence of CB1R in the monkey retina is well established (Straiker et al., 1999;

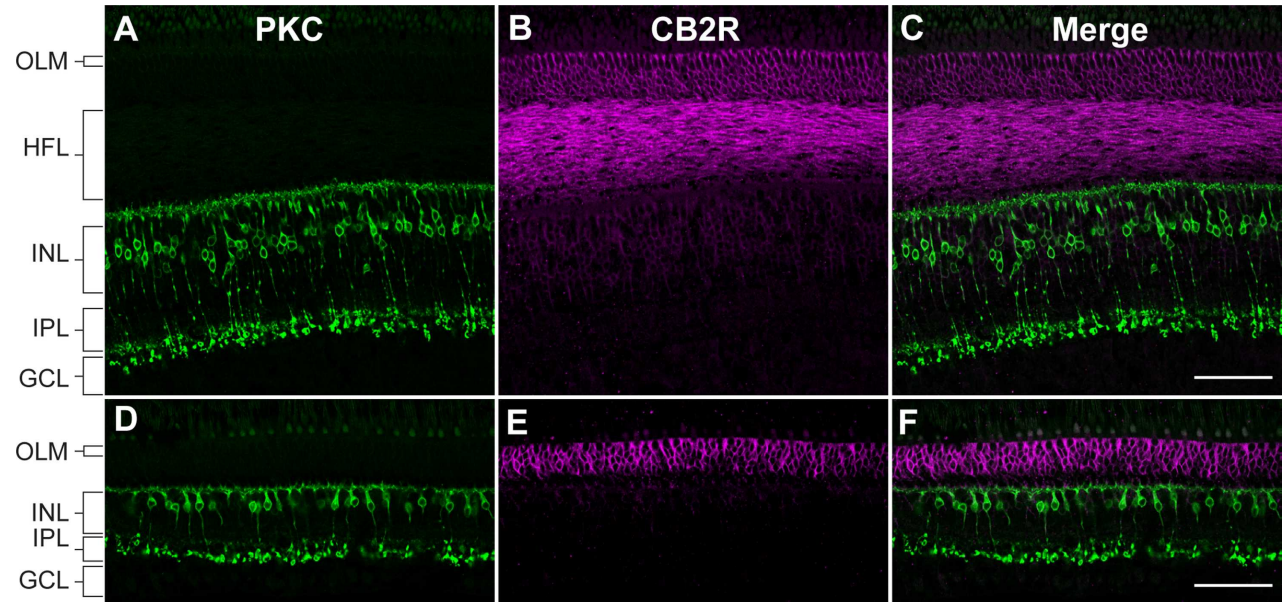

Figure 5. Double-label immunofluorescence illustrating the localization of PKC and CB2R. A–F: Vertical sections showing PKC-positive fibers representing rod bipolar cell axons that appear colocalized near the fovea (**A, B**) and in the middle retina (**D–F**). CB2R-IR followed the Müller cell processes, insinuating themselves between cell bodies of the neurons in the inner nuclear layer. No PKC-immunoreactive cell was CB2R immunoreactive. OLM, outer limiting membrane; HFL, Henle fiber layer; INL, inner nuclear layer; IPL, inner plexiform layer; GCL, ganglion cell layer. Scale bars = 75 μm in C (applies to A–C); 75 μm in F (applies to D–F). [Color figure can be viewed in the online issue, which is available at wileyonlinelibrary.com]

Bouskila et al., 2012), we are still far from identifying the exact role of eCB signaling in the monkey retina. Furthermore, CB2R has been previously ascribed a critical role in CNS glial function (Cabral et al., 2008), and its visual function remains elusive. Our aim was to characterize further the retinal localization of cannabinoid receptors, especially by comparing the CB2R expression profile with CB1R localization. We demonstrate here that CB2R is present in the retina of the vervet monkey and specifically in retinal Müller cells.

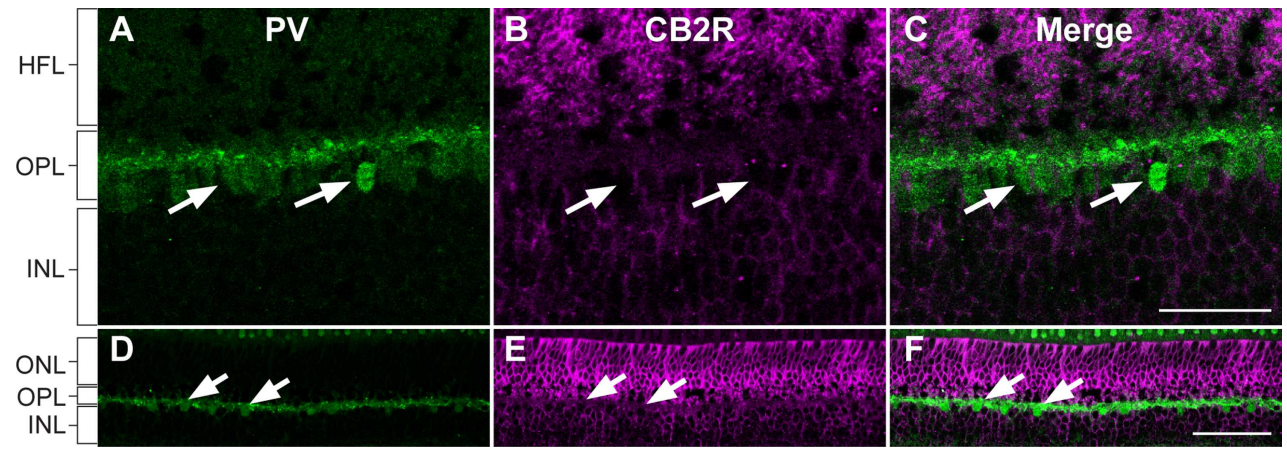

Figure 6. Localization of parvalbumin (PV) and CB2R within the central and peripheral retina. Note that the CB2R labeling (magenta) is not located within PV-immunoreactive horizontal cell somata and processes (green). High-magnification images of PV, CB2R, and merged views, respectively, in the central retina (**A–C**) and in the middle retina (**D–F**). Occasional CB2R-immunoreactive fibers in the OPL surround the horizontal cell somata (arrows). HFL, Henle fiber layer; ONL, outer nuclear layer; OPL, outer plexiform layer; INL, inner nuclear layer. Scale bar = 37.5 μm in C (applies to A–C); 75 μm in F (applies to D–F). [Color figure can be viewed in the online issue, which is available at wileyonlinelibrary.com]

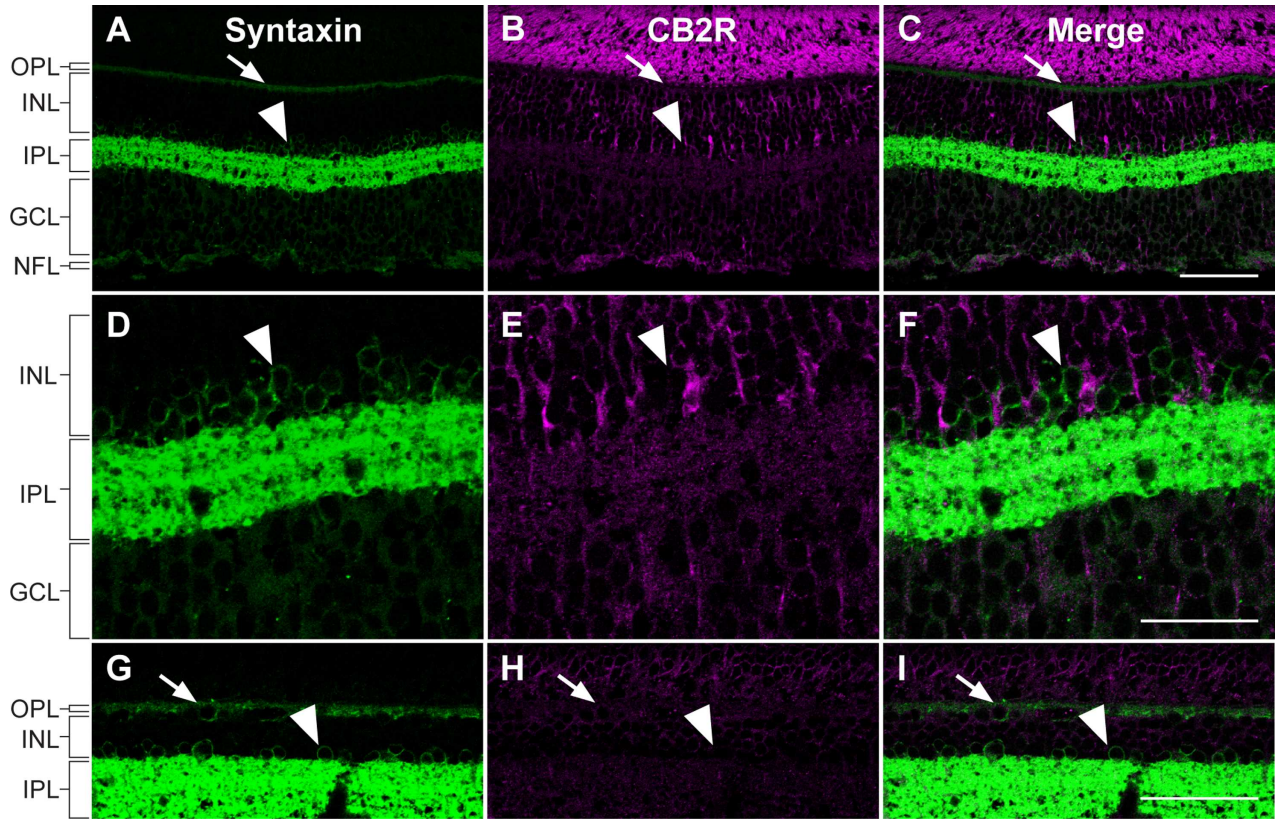

Figure 7. Double-label immunofluorescence illustrating the localization of syntaxin (green) and CB2R (magenta) in the monkey retina. **A–C:** Syntaxin-immunoreactive horizontal (arrows) and amacrine cells (arrowheads) were clearly not labeled with CB2R in the central retina. **D–F:** Higher magnification of syntaxin-IR and CB2R-IR in the central retina. **G–I:** Syntaxin-IR and CB2R-IR in the middle retina. Syntaxin-IR labeled heavily the membrane of horizontal cells in the OPL but lightly their cytosol and also labeled heavily the membrane of amacrine cells and IPL but lightly their cytosol. OPL, outer plexiform layer; INL, inner nuclear layer; IPL, inner plexiform layer; GCL, ganglion cell layer; NFL, nerve fiber layer. Scale bars = 75 μm in C (applies to A–C); 37.5 μm in F (applies to D–F); 75 μm in I (applies to G–I). [Color figure can be viewed in the online issue, which is available at wileyonlinelibrary.com]

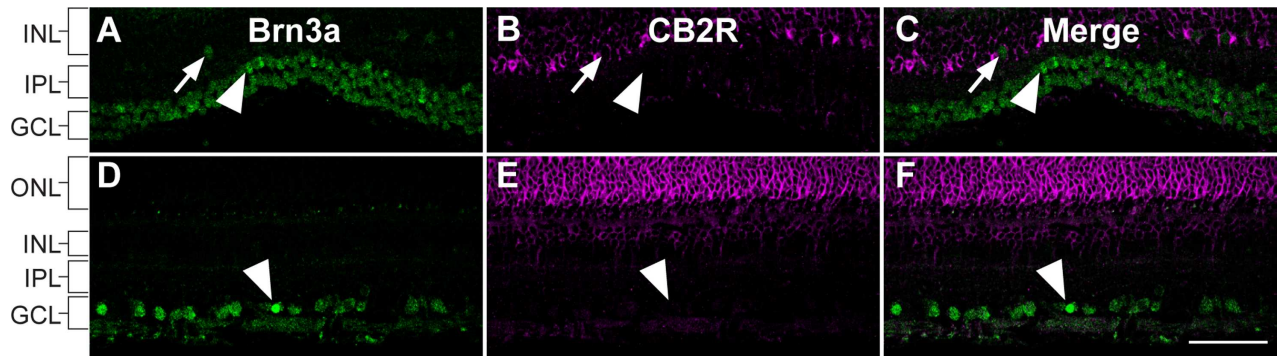

Figure 8. Double-label immunofluorescence illustrating localization of CB2R (magenta) and Brn3a (green) in the central retina (**A–C**) and in the middle retina (**D–F**). The antibody against Brn3a labels the nucleus of ganglion cells in the monkey retina, and these cells were not CB2R immunoreactive. The occasional labeling of CB2R in the ganglion cell layer was localized in the Müller cells inner processes. Arrows point to a Brn3a-positive cell that is not localized in the GCL, and arrowheads indicate Brn3a-positive ganglion cells that are not CB2R immunoreactive. ONL, outer nuclear layer; INL, inner nuclear layer; IPL, inner plexiform layer; GCL, ganglion cell layer. Scale bar = 75 μm. [Color figure can be viewed in the online issue, which is available at wileyonlinelibrary.com]

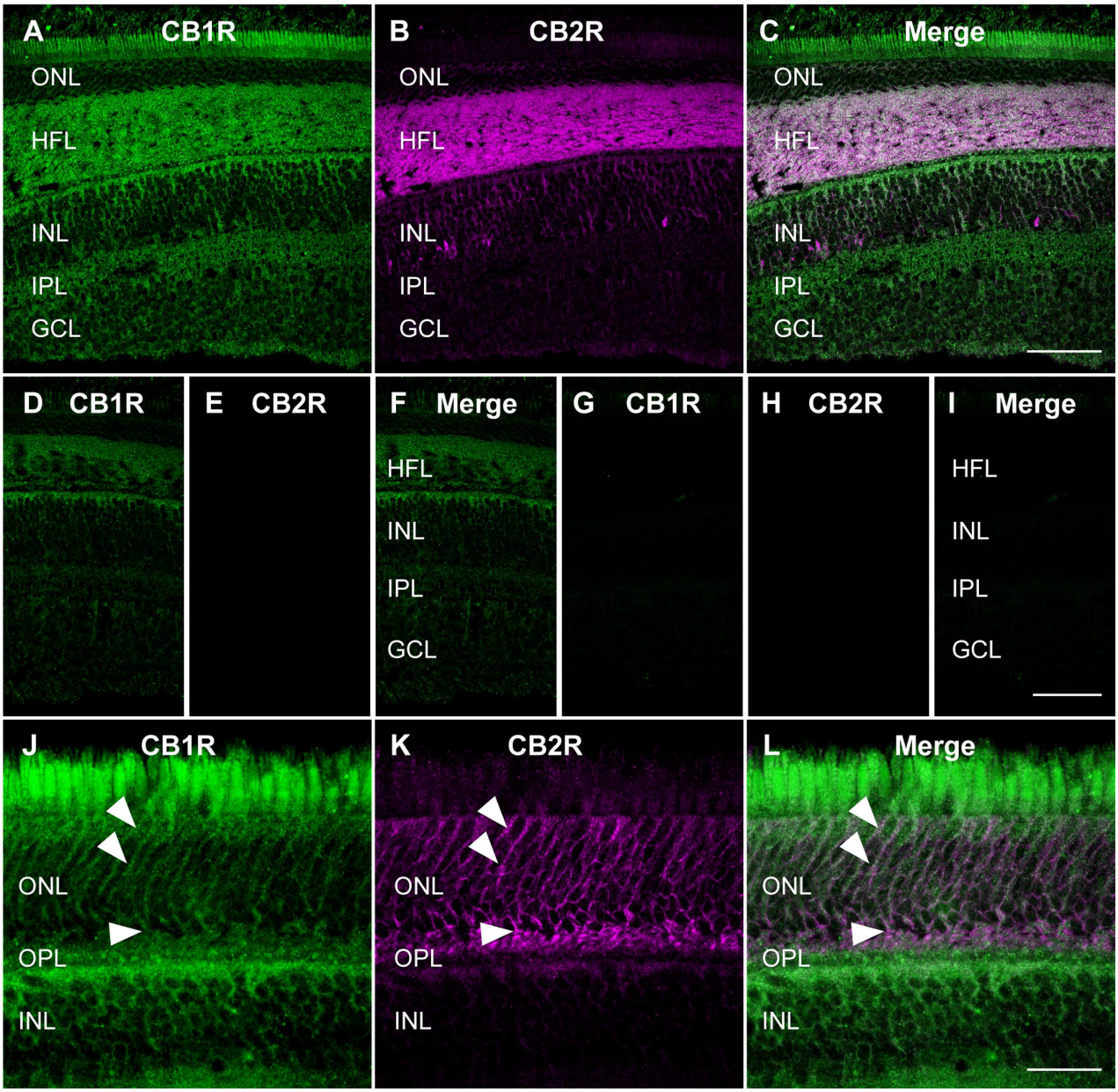

Figure 9. Comparison of CB1R and CB2R retinal expressions. Confocal micrographs of retinae co-immunolabeled for CB1R (green) and CB2R (magenta). CB1R (**A, D, G, J**) and CB2R (**B, E, H, K**) signals and their overlay (**C, F, I, L**). A–C: Complete sequential protocol in the central retina. D–F: The second primary antibody was omitted. G–I: The first secondary and second primary antibodies were lacking. J–L: Localization of CB1R and CB2R in the outer retina. Arrowheads follow a CB1R-positive cone cell body and axon, and CB2R-positive Müller cells processes that enroll this cone. ONL, outer nuclear layer; HFL, Henle fiber layer; INL, inner nuclear layer; IPL, inner plexiform layer; GCL, ganglion cell layer. Scale bars = 75 μm in C (applies to A–C); 75 μm in I (applies to D–I); 75 μm in L (applies to J–L). [Color figure can be viewed in the online issue, which is available at wileyonlinelibrary.com]

These data, in agreement with CB2R glial expression in the CNS, suggest that the CB2 receptor plays a role in retinal functions.

There are three types of glial cells in the primate retina: Müller cells, astrocytes, and microglia. Müller cells are the principal glial cells of the retina and are radially oriented across the thickness of the retina, analogous to CB2R expression profile in the distal retina. Their processes extend from the outer limiting membrane to the inner limiting membrane. Given that the expression of the CB2R followed the same pattern, with a higher polarization towards the outer retina, we suggest that CB2R is localized in these glial cells, verified by the colocalization of CB2R-IR with GS-IR. Müller cell processes surround neuronal cell bodies in the nuclear layers and envelop groups of neural processes in the

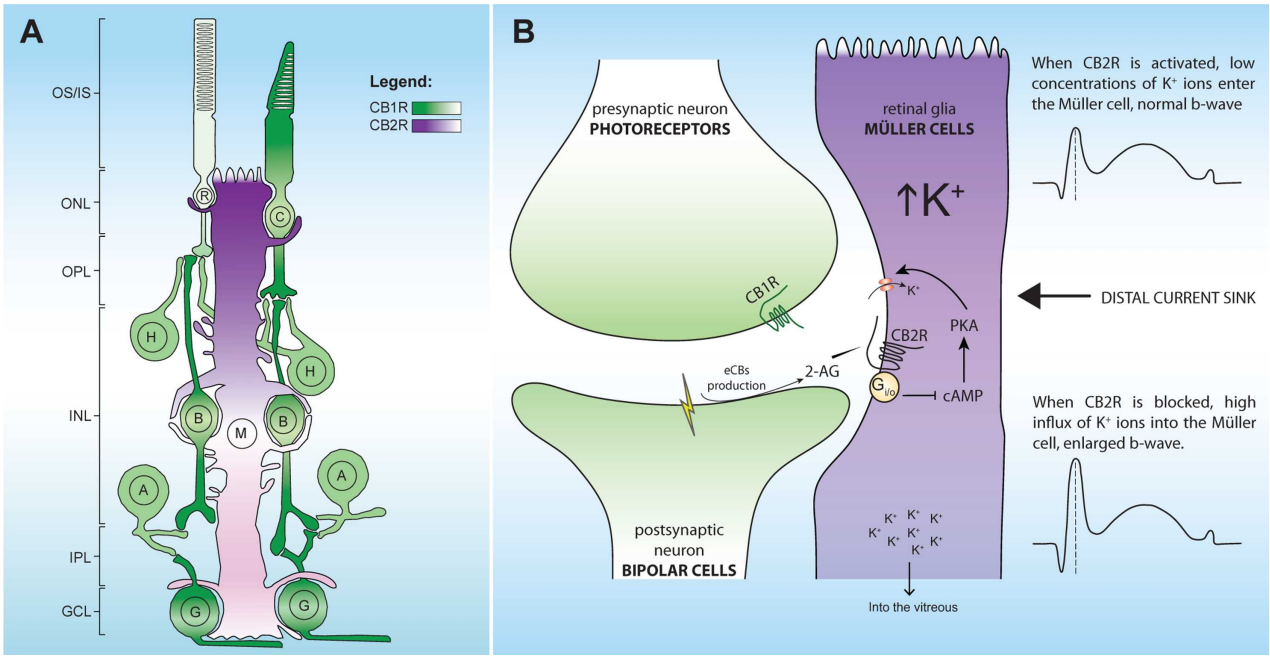

Figure 10. Schematic illustration representing the localization of the principal cannabinoid receptors (**A**) and a hypothetical function for CB2R (**B**) in the monkey retina. CB1R is localized in neural components and CB2R in glial components (Müller cells). Color bars in the key indicate the intensity of CB1R (green) and CB2R (magenta) expressions. OS/IS, outer and inner segments of rods and cones; ONL, outer nuclear layer; OPL, outer plexiform layer; INL, inner nuclear layer; IPL, inner plexiform layer; GCL, ganglion cell layer; C, cones; R, rods; H, horizontal cells; B, bipolar cells; A, amacrine cells; G, retinal ganglion cells; M, Müller cells. [Color figure can be viewed in the online issue, which is available at wileyonlinelibrary.com]

plexiform layers. A 3D visualization was therefore needed to determine whether CB2R-IR was present in neurons. The outer limiting membrane (OLM), which represents the outer border of CB2R expression, is composed of junctions among Müller cells and photoreceptor cells. However, CB2R-IR was not detected in the apical villi of Müller cells that extend distally from the OLM. The inner limiting membrane, formed by the conical endfeet of Müller cells, appeared devoid of CB2R-IR. Müller cells also form endfeet on the large retinal blood vessels at the inner surface of the retina. Given the apparent absence of CB2R-IR in the most proximal retina, CB2R may not have a role in the regulation of inner retinal blood vessels.

The presence of CB2R in Müller cells and CB1R in the retinal neuronal cells points toward a complementary relationship between neurons and glia regarding endocannabinoid function. CB2R in Müller cells could protect neurons from exposure to excess neurotransmitters such as L-glutamate (Placzek et al., 2008). Generally, CB2R activation leads to sequences of activities of a protective nature (for review see Pacher and Mechoulam, 2011). Stimulation of CB2R increases microglial cell proliferation (Carrier et al., 2004) and reduces the release of harmful factors, including tumor necrosis factor (TNF) and free radicals (Ramírez et al., 2005; Eljaschewitsch et al., 2006; for review see Stella, 2009). In fact, exposure to eCBs in activated primary human Müller glia inhibited the production of several proinflammatory cytokines (Krishnan and Chatterjee, 2012). CB2R in Müller cells might therefore be an important player in inflammation, neurotoxicity, and neuroprotection. The localization of CB1R in the photoreceptor layer already suggested that the transduction of light (Yazulla, 2008) occurring at this stage could also be modulated by the CB2R expressed in distal Müller cells fibers. Perhaps the whole eCB system participates in the modulation of light transduction, where CB1R is neuronal and CB2R glial. The expression of CB1R in bipolar cells, shown by double labeling with CHX10 and PKC retinal cell type markers, suggested that the eCB system acts as an autoregulation system that modulates the signal received by the photoreceptors in order to transmit it to ganglion cells (Yazulla et al., 1999; Yazulla, 2008; Bouskila et al., 2012). Similarly, this could also occur in horizontal and amacrine cells that show little expression of CB1R (Bouskila et al., 2012). Finally, it is possible that the results of Lu et al. (2000), who demonstrated the expression of CB2R in the ganglion cell layer of the adult rat retina

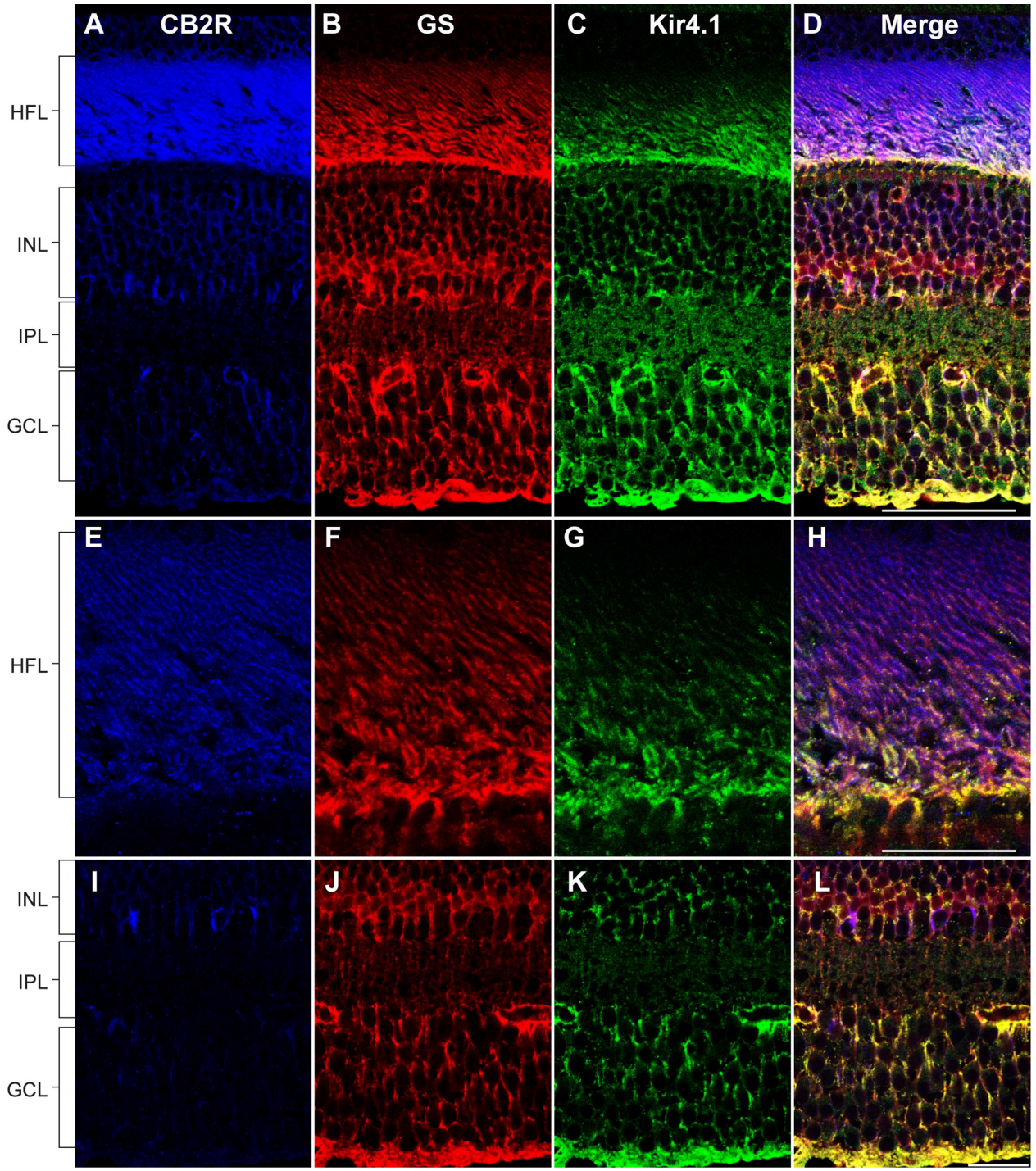

Figure 11. Triple-immunofluorescence labeling of CB2R, glutamine synthetase (GS), and the potassium ion channel Kir4.1 in the monkey central retina. Each protein is presented alone in the first columns. The merged images are presented in the last column (CB2R in blue, GS in red, and Kir4.1 in green). **A–D:** Low-magnification images showing Kir4.1 and CB2R expression in GS-positive Müller cells. **E–H:** High-magnification images of Kir4.1, CB2R, and GS immunoreactivity in the distal retina showing colocalization of CB2R and Kir4.1 in Müller cell fibers of the Henle fiber layer. **I–L:** High-magnification images of Kir4.1 expression in the proximal retina. HFL, Henle fiber layer; INL, inner nuclear layer; IPL, inner plexiform layer; GCL, ganglion cell layer. Scale bars = 75 μm in D (applies to A–D); 30 μm in H (applies to E–H); 30 μm in L (applies to I–L). [Color figure can be viewed in the online issue, which is available at wileyonlinelibrary.com]

using in situ hybridization and RT-PCR, did include CB2R-immunoreactive Müller cell processes. In agreement with the latter study, using immunohistochemistry and cell morphology, López et al. (2011) suggested that CB2R was localized in photoreceptors, horizontal cells, amacrine cells, and cells localized in the GCL of the

adult rat retina. These studies differ with ours regarding not only the animal model (rat vs. monkey) but also the choice of the antibody used. Although we used an antibody targeted against the 20–33 amino acids of the human CB2R, López et al. (2011) used an antibody against residues 326–342 of the rat CB2R. Moreover, double labeling of CB2R with a retinal cell marker was not performed, and, given that Müller cells envelop the cell bodies in the GCL, it could be CB2R-positive cells. In addition, CB1R-IR in the Henle fiber layer and ganglion cell layer of the monkey retina has the most prominent staining found throughout the retinal layers (Bouskila et al., 2012), as opposed to only the Henle fiber layer that has the highest CB2R signal. Recently, Krishnan and Chatterjee (2012) showed that CB2R protein was expressed in homogenates of 12–18 days ex vivo retinal explants and 18 days in vitro primary Müller glia from human retina by Western blotting. Here we provide direct evidence for the in vivo expression pattern of CB2R in monkey Müller cells by immunohistochemistry.

HYPOTHETICAL FUNCTIONAL CONSEQUENCES

Activation of photoreceptors by light evokes an increase of K^+ ions in the retinal extracellular space (Newman and Reichenbach, 1996). To maintain an electrolytic balance, Müller cell inwardly rectifying K^+ channels (K_{IR}) release the excess K^+ ions into the vitreous. This spatial buffering mechanism is termed *K^+ siphoning* (Newman et al., 1984). Immunoreactivity to the $K_{IR}4.1$ channel in rat retina was densely distributed around photoreceptor cells in ONL, where the distal ends of Müller cells surround PR cells, and in a scattered manner around ganglion cells in GCL in rat retina (Ishii et al., 1997). Interestingly, $K_{IR}4.1$-IR as reported by Ishii et al. (1997) for the rodent retina is similar to CB2R expression found in Müller cells in the present study in the monkey central retina (Fig. 11). The cellular origin of the b-wave component of the ERG is attributed to an interaction between On-bipolar cells and Müller cells (Stockton and Slaughter, 1989; Wen and Oakley, 1990). The b-wave of the ERG reflects the K^+-mediated spatial buffering currents of Müller cells (Miller and Dowling, 1970; Kline et al., 1985). Moreover, blocking K^+ channels in Müller cells reduces the ERG b-wave (Wen and Oakley, 1990). Given that activation of CB2R leads to a reduction of cAMP and PKA levels as a result of coupling via $G_{i/o}$ (Howlett et al., 2002; for review see Bolognini et al., 2010) and that PKA increases the activity of $K_{IR}4.1$ channels in Müller cells (MacGregor et al., 1998), it is reasonable to propose that CB2R plays a role in the generation of the b-wave. CB2R could act therefore as a negative modulator of K^+ channels. Conversely, blocking CB2R activates K^+ channels (because of the constitutive activity of CB2R) that in turn produces a constant influx of K^+ ions into the Müller cell and an enlarged b-wave (Fig. 10B). Further experiments are still needed to verify this putative retinal CB2R function.

ACKNOWLEDGMENTS

We thank Sophie Charron and Florence Dotigny for excellent technical assistance. We are grateful to Dr. Frank Ervin and Dr. Roberta Palmour of the Behavioral Sciences Foundation Laboratories of St.-Kitts, West Indies, for supplying the vervet monkey tissues. J.B. holds a scholarship from "Fonds de recherche du Québec–Santé (FRQS)." M.P. is Harland Sanders Chair Professor in Visual Science. J.-F.B. is supported by a "Chercheur-Boursier Junior 2" from FRQS.

CONFLICT OF INTEREST STATEMENT

The authors declare no conflicts of interest.

ROLE OF AUTHORS

All authors had full access to all the data in the study and take responsibility for the integrity of the data and the accuracy of the data analysis. Study concept and design: JB. Acquisition of data: JB. Analysis and interpretation of data: JB. Drafting of the manuscript: JB and PJ. Critical revision of the manuscript for important intellectual content: CC. Obtained funding: CC, MP, and J-FB. Administrative, technical, and material support: CC, MP and J-FB. Study supervision: MP and J-FB.

LITERATURE CITED

Argaw A, Duff G, Cherif H, Cécyre B, Tea N, and Bouchard J-F. 2011. Cannabinoid receptor CB2 modulates axon guidance. Abstract B045, 8th IBRO World Congress on Neuroscience, Firenze, Italy.

Atwood BK, Mackie K. 2010. CB2: a cannabinoid receptor with an identity crisis. Br J Pharmacol 160:467–479.

Barnstable CJ, Hofstein R, Akagawa K. 1985. A marker of early amacrine cell development in rat retina. Brain Res 352:286–290.

Bolognini D, Costa B, Maione S, Comelli F, Marini P, Di Marzo V, Parolaro D, Ross RA, Gauson LA, Cascio MG, Pertwee RG. 2010. The plant cannabinoid delta9-tetrahydrocannabivarin can decrease signs of inflammation and inflammatory pain in mice. Br J Pharmacol 160:677–687.

Bordt A, Hoshi H, Yamada E, Perryman Stout W, Marshak D. 2006. Synaptic input to Off parasol ganglion cells in macaque retina. J Comp Neurol 498:46–57.

Bouskila J, Burke MW, Zabouri N, Casanova C, Ptito M, Bouchard JF. 2012. Expression and localization of the cannabinoid receptor type 1 and the enzyme fatty acid amide

hydrolase in the retina of vervet monkeys. Neuroscience 202:117–130.
Brandon C. 1985. Improved immunocytochemical staining through the use of Fab fragments of primary antibody, Fab-specific second antibody, and Fab-horseradish peroxidase. J Histochem Cytochem 33:715–719.
Buckley NE, Hansson S, Harta G, Mezey E. 1998. Expression of the CB1 and CB2 receptor messenger RNAs during embryonic development in the rat. Neuroscience 82:1131–1149.
Burke M, Zangenehpour S, Bouskila J, Boire D, Ptito M. 2009. The gateway to the brain: dissecting the primate eye. J Vis Exp e1261.
Cabral GA, Raborn ES, Griffin L, Dennis J, Marciano-Cabral F. 2008. CB2 receptors in the brain: role in central immune function. Br J Pharmacol 153:240–251.
Carrier EJ, Kearn CS, Barkmeier AJ, Breese NM, Yang W, Nithipatikom K, Pfister SL, Campbell WB, Hillard CJ. 2004. Cultured rat microglial cells synthesize the endocannabinoid 2-arachidonylglycerol, which increases proliferation via a CB2 receptor-dependent mechanism. Mol Pharmacol 65:999–1007.
Chen J, Matias I, Dinh T, Lu T, Venezia S, Nieves A, Woodward DF, Di Marzo V. 2005. Finding of endocannabinoids in human eye tissues: implications for glaucoma. Biochem Biophys Res Commun 330:1062–1067.
Chiquet C, Dkhissi-Benyahya O, Chounlamountri N, Szel A, Degrip WJ, Cooper HM. 2002. Characterization of calbindin-positive cones in primates. Neuroscience 115:1323–1333.
Cravatt BF, Giang DK, Mayfield SP, Boger DL, Lerner RA, Gilula NB. 1996. Molecular characterization of an enzyme that degrades neuromodulatory fatty-acid amides. Nature 384:83–87.
Cuenca N, Herrero MT, Angulo A, de Juan E, Martínez-Navarrete GC, López S, Barcia C, Martín-Nieto J. 2005. Morphological impairments in retinal neurons of the scotopic visual pathway in a monkey model of Parkinson's disease. J Comp Neurol 493:261–273.
Devane WA, Hanus L, Breuer A, Pertwee RG, Stevenson LA, Griffin G, Gibson D, Mandelbaum A, Etinger A, Mechoulam R. 1992. Isolation and structure of a brain constituent that binds to the cannabinoid receptor. Science 258:1946–1949.
Di Marzo V, Bisogno T, De Petrocellis L. 2007. Endocannabinoids and related compounds: walking back and forth between plant natural products and animal physiology. Chem Biol 14:741–756.
Dinh TP, Carpenter D, Leslie FM, Freund TF, Katona I, Sensi SL, Kathuria S, Piomelli D. 2002. Brain monoglyceride lipase participating in endocannabinoid inactivation. Proc Natl Acad Sci U S A 99:10819–10824.
Distler C, Dreher Z. 1996. Glia cells of the monkey retina–II. Müller cells. Vis Res 36:2381–2394.
Eljaschewitsch E, Witting A, Mawrin C, Lee T, Schmidt P, Wolf S, Hoertnagl H, Raine C, Schneider Stock R, Nitsch R, Ullrich O. 2006. The endocannabinoid anandamide protects neurons during CNS inflammation by induction of MKP-1 in microglial cells. Neuron 49:67–79.
Ellert-Miklaszewska A, Grajkowska W, Gabrusiewicz K, Kaminska B, Konarska L. 2007. Distinctive pattern of cannabinoid receptor type II (CB2) expression in adult and pediatric brain tumors. Brain Res 1137:161–169.
Fischer AJ, Hendrickson A, Reh TA. 2001. Immunocytochemical characterization of cysts in the peripheral retina and pars plana of the adult primate. Invest Ophthalmol Vis Sci 42:3256–3263.
Galiègue S, Mary S, Marchand J, Dussossoy D, Carrière D, Carayon P, Bouaboula M, Shire D, Le Fur G, Casellas P. 1995. Expression of central and peripheral cannabinoid receptors in human immune tissues and leukocyte subpopulations. Eur J Biochem 232:54–61.
Griffin G, Tao Q, Abood ME. 2000. Cloning and pharmacological characterization of the rat CB2 cannabinoid receptor. J Pharmacol Exp Ther 292:886–894.
Howlett AC, Barth F, Bonner TI, Cabral G, Casellas P, Devane WA, Felder CC, Herkenham M, Mackie K, Martin BR, Mechoulam R, Pertwee RG. 2002. International Union of Pharmacology. XXVII. Classification of cannabinoid receptors. Pharmacol Rev 54:161–202.
Inoue A, Obata K, Akagawa K. 1992. Cloning and sequence analysis of cDNA for a neuronal cell membrane antigen, HPC-1. J Biol Chem 267:10613–10619.
Ishii M, Horio Y, Tada Y, Hibino H, Inanobe A, Ito M, Yamada M, Gotow T, Uchiyama Y, Kurachi Y. 1997. Expression and clustered distribution of an inwardly rectifying potassium channel, KAB-2/Kir4.1, on mammalian retinal Müller cell membrane: their regulation by insulin and laminin signals. J Neurosci 17:7725–7735.
Kline RP, Ripps H, Dowling JE. 1985. Light-induced potassium fluxes in the skate retina. Neuroscience 14:225–235.
Kolb H, Zhang L, Dekorver L, Cuenca N. 2002. A new look at calretinin-immunoreactive amacrine cell types in the monkey retina. J Comp Neurol 453:168–184.
Kozak KR, Rowlinson SW, Marnett LJ. 2000. Oxygenation of the endocannabinoid, 2-arachidonylglycerol, to glyceryl prostaglandins by cyclooxygenase-2. J Biol Chem 275:33744–33749.
Krishnan G, Chatterjee N. 2012. Endocannabinoids alleviate proinflammatory conditions by modulating innate immune response in Müller glia during inflammation. Glia 60:1629–1645.
Li L, Head V, Timpe LC. 2001. Identification of an inward rectifier potassium channel gene expressed in mouse cortical astrocytes. Glia 33:57–71.
López EM, Tagliaferro P, Onaivi ES, López-Costa JJ. 2011. Distribution of CB2 cannabinoid receptor in adult rat retina. Synapse 65:388–392.
Lu Q, Straiker A, Maguire G. 2000. Expression of CB2 cannabinoid receptor mRNA in adult rat retina. Vis Neurosci 17:91–95.
MacGregor GG, Xu JZ, McNicholas CM, Giebisch G, Hebert SC. 1998. Partially active channels produced by PKA site mutation of the cloned renal K^+ channel, ROMK2 (kir1.2). Am J Physiol 275:F415–F422.
Mackie K. 2008. Cannabinoid receptors: where they are and what they do. J Neuroendocrinol 20(Suppl 1):10–14.
Martínez-Navarrete GC, Martín-Nieto J, Esteve-Rudd J, Angulo A, Cuenca N. 2007. Alpha synuclein gene expression profile in the retina of vertebrates. Mol Vis 13:949–961.
Martínez-Navarrete GC, Angulo A, Martín-Nieto J, Cuenca N. 2008. Gradual morphogenesis of retinal neurons in the peripheral retinal margin of adult monkeys and humans. J Comp Neurol 511:557–580.
McPartland JM, Norris RW, Kilpatrick CW. 2007. Coevolution between cannabinoid receptors and endocannabinoid ligands. Gene 397:126–135.
Mechoulam R, Ben Shabat S, Hanus L, Ligumsky M, Kaminski NE, Schatz AR, Gopher A, Almog S, Martin BR, Compton DR. 1995. Identification of an endogenous 2-monoglyceride, present in canine gut, that binds to cannabinoid receptors. Biochem Pharmacol 50:83–90.
Miller RF, Dowling JE. 1970. Intracellular responses of the Müller (glial) cells of mudpuppy retina: their relation to b-wave of the electroretinogram. J Neurophysiol 33:323–341.
Mills SL, Massey SC. 1999. AII amacrine cells limit scotopic acuity in central macaque retina: a confocal analysis of calretinin labeling. J Comp Neurol 411:19–34.

Mukherjee S, Adams M, Whiteaker K, Daza A, Kage K, Cassar S, Meyer M, Yao BB. 2004. Species comparison and pharmacological characterization of rat and human CB2 cannabinoid receptors. Eur J Pharmacol 505:1–9.

Munro S, Thomas KL, Abu-Shaar M. 1993. Molecular characterization of a peripheral receptor for cannabinoids. Nature 365:61–65.

Nadal-Nicolás FM, Jiménez-López M, Sobrado-Calvo P, Nieto-López L, Cánovas-Martínez I, Salinas-Navarro M, Vidal-Sanz M, Agudo M. 2009. Brn3a as a marker of retinal ganglion cells: qualitative and quantitative time course studies in naïve and optic nerve-injured retinas. Invest Ophthalmol Vis Sci 50:3860–3868.

Nag TC, Wadhwa S. 2001. Differential expression of syntaxin-1 and synaptophysin in the developing and adult human retina. J Biosci 26:179–191.

Newman E, Reichenbach A. 1996. The Müller cell: a functional element of the retina. Trends Neurosci 19:307–312.

Newman EA, Frambach DA, Odette LL. 1984. Control of extracellular potassium levels by retinal glial cell K^+ siphoning. Science 225:1174–1175.

Nishikawa S, Tamai M. 2001. Müller cells in the human foveal region. Curr Eye Res 22:34–41.

Onaivi E, Ishiguro H, Gu S, Liu Q-R. 2012. CNS effects of CB2 cannabinoid receptors: beyond neuro-immuno-cannabinoid activity. J Psychopharmacol 26:92–103.

Pacher P, Mechoulam R. 2011. Is lipid signaling through cannabinoid 2 receptors part of a protective system? Prog Lipid Res 50:193–211.

Piomelli D. 2003. The molecular logic of endocannabinoid signalling. Nat Rev Neurosci 4:873–884.

Placzek EA, Okamoto Y, Ueda N, Barker EL. 2008. Mechanisms for recycling and biosynthesis of endogenous cannabinoids anandamide and 2-arachidonylglycerol. J Neurochem 107:987–1000.

Porcella A, Casellas P, Gessa GL, Pani L. 1998. Cannabinoid receptor CB1 mRNA is highly expressed in the rat ciliary body: implications for the antiglaucoma properties of marihuana. Brain Res Mol Brain Res 58:240–245.

Porcella A, Maxia C, Gessa GL, Pani L. 2000. The human eye expresses high levels of CB1 cannabinoid receptor mRNA and protein. Eur J Neurosci 12:1123–1127.

Qi H-X, Gharbawie OA, Wong P, Kaas JH. 2011. Cell-poor septa separate representations of digits in the ventroposterior nucleus of the thalamus in monkeys and prosimian galagos. J Comp Neurol 519:738–758.

Ramírez BG, Blázquez C, del Pulgar TG, Guzmán M, de Ceballos ML. 2005. Prevention of Alzheimer's disease pathology by cannabinoids: neuroprotection mediated by blockade of microglial activation. J Neurosci 25: 1904–1913.

Riepe RE, Norenburg MD. 1977. Müller cell localisation of glutamine synthetase in rat retina. Nature 268:654–655.

Röhrenbeck J, Wässle H, Heizmann CW. 1987. Immunocytochemical labelling of horizontal cells in mammalian retina using antibodies against calcium-binding proteins. Neurosci Lett 77:255–260.

Shire D, Calandra B, Rinaldi-Carmona M, Oustric D, Pessègue B, Bonnin-Cabanne O, Le Fur G, Caput D, Ferrara P. 1996. Molecular cloning, expression and function of the murine CB2 peripheral cannabinoid receptor. Biochim Biophys Acta 1307:132–136.

Stella N. 2009. Endocannabinoid signaling in microglial cells. Neuropharmacology 56(Suppl 1):244–253.

Stockton RA, Slaughter MM. 1989. B-wave of the electroretinogram. A reflection of ON bipolar cell activity. J Gen Physiol 93:101–122.

Straiker A, Stella N, Piomelli D, Mackie K, Karten HJ, Maguire G. 1999. Cannabinoid CB1 receptors and ligands in vertebrate retina: localization and function of an endogenous signaling system. Proc Natl Acad Sci U S A 96:14565–14570.

Sugiura T, Kondo S, Sukagawa A, Nakane S, Shinoda A, Itoh K, Yamashita A, Waku K. 1995. 2-Arachidonoylglycerol: a possible endogenous cannabinoid receptor ligand in brain. Biochem Biophys Res Commun 215:89–97.

Wässle H, Dacey DM, Haun T, Haverkamp S, Grunert U, Boycott BB. 2000. The mosaic of horizontal cells in the macaque monkey retina: with a comment on biplexiform ganglion cells. Vis Neurosci 17:591–608.

Wei Y, Wang X, Wang L. 2009. Presence and regulation of cannabinoid receptors in human retinal pigment epithelial cells. Mol Vis 15:1243–1251.

Wen R, Oakley B 2nd. 1990. K^+-evoked Müller cell depolarization generates b-wave of electroretinogram in toad retina. Proc Natl Acad Sci U S A 87:2117–2121.

Xiang M, Zhou L, Macke JP, Yoshioka T, Hendry SH, Eddy RL, Shows TB, Nathans J. 1995. The Brn-3 family of POU-domain factors: primary structure, binding specificity, and expression in subsets of retinal ganglion cells and somatosensory neurons. J Neurosci 15:4762–4785.

Yazulla S. 2008. Endocannabinoids in the retina: from marijuana to neuroprotection. Prog Ret Eye Res 27:501–526.

Yazulla S, Studholme KM, McIntosh HH, Deutsch DG. 1999. Immunocytochemical localization of cannabinoid CB1 receptor and fatty acid amide hydrolase in rat retina. J Comp Neurol 415:80–90.

Zabouri N, Bouchard JF, Casanova C. 2011a. Cannabinoid receptor type 1 expression during postnatal development of the rat retina. J Comp Neurol 519:1258–1280.

Zabouri N, Ptito M, Casanova C, Bouchard JF. 2011b. Fatty acid amide hydrolase expression during retinal postnatal development in rats. Neuroscience 195:145–165.

Zhong L, Geng L, Njie Y, Feng W, Song Z-H. 2005. CB2 cannabinoid receptors in trabecular meshwork cells mediate JWH015-induced enhancement of aqueous humor outflow facility. Invest Ophthalmol Vis Sci 46:1988–1992.

Zurolo E, Iyer AM, Spliet WGM, Van Rijen PC, Troost D, Gorter JA, Aronica E. 2010. CB1 and CB2 cannabinoid receptor expression during development and in epileptogenic developmental pathologies. Neuroscience 170:28–41.